Chapter 6 Bulk Nanostructured Materials

- Bulk nanostructured materials are solid
- having
- 1. a nanosized microstructure
- 2. the basic units are nanoparticles

Hypothetical 2-D Oedered –Al_{12} particles forming nanostructure

Disordered Al_{12} Particles

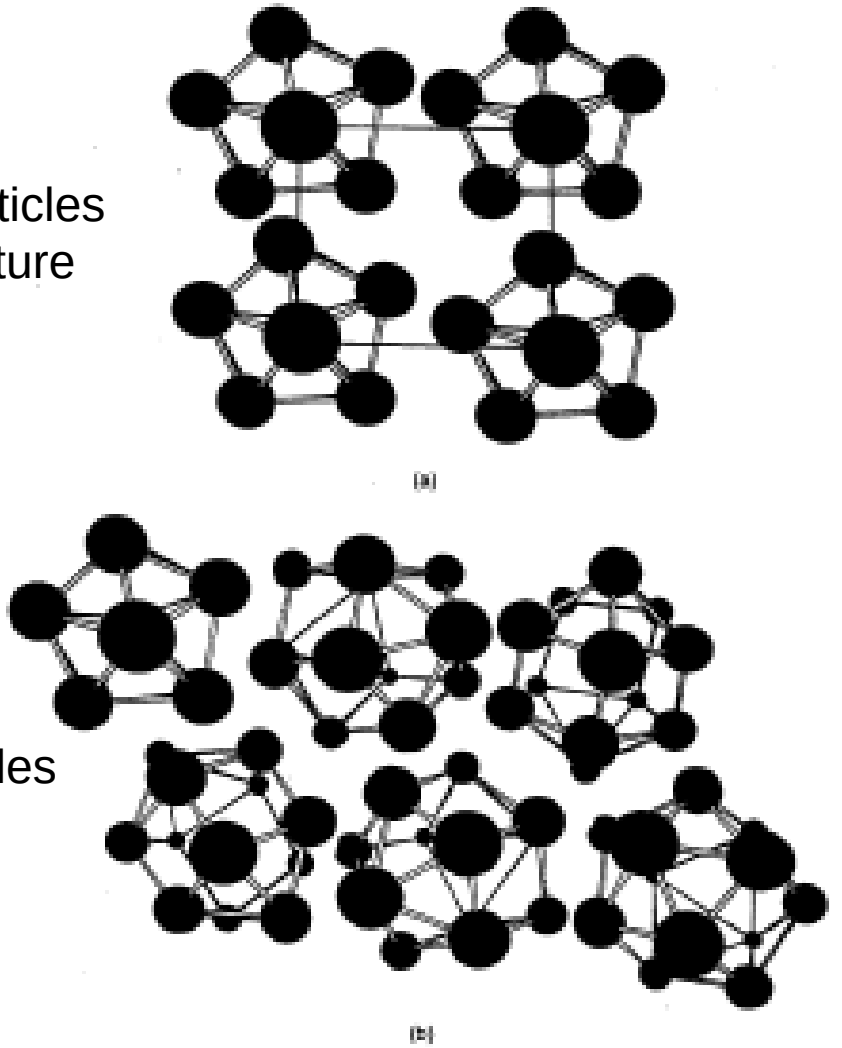

Figure 6.1. (a) Illustration of a hypothetical two-dimensional square lattice of Al_{12} particles, and (b) illustration of a two-dimensional bulk solid of Al_{12} where the nanoparticles have no ordered arrangement with respect to each other.

6.1 Solid disordersed nanostructure

- Compaction and consolidation
- 1. 85%Cu and 15%Fe powder in atomic weight
- 2. Ball milling to form $Fe_{85}Cu_{15}$ particles
- 3. Compacted using a tungsten-carbide at 1GPa for 24 h
- 4. Hot compaction at ~ 400C with 870 MPa
- 5. Final density 99.2%

Distribution of size

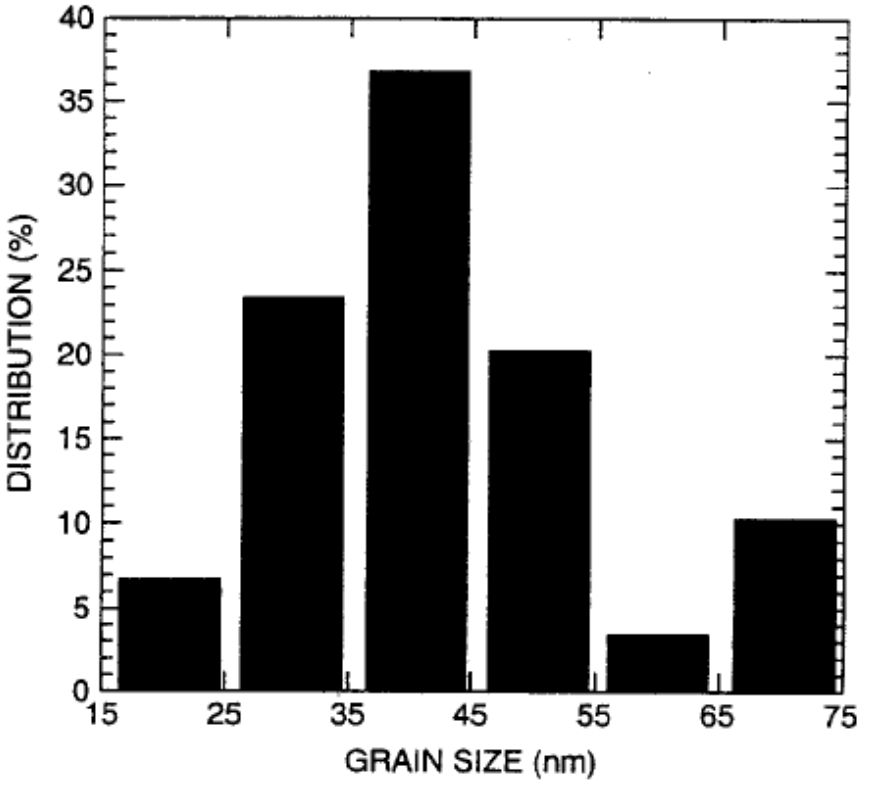

Figure 6.2. Distribution of sizes of Fe–Cu nanoparticles made by hot compaction methods described in the text. [Adapted from L. He and E. Ma, *J. Mater. Res.* **15**, 904 (2000).]

$CeAl_2$ HRTEM

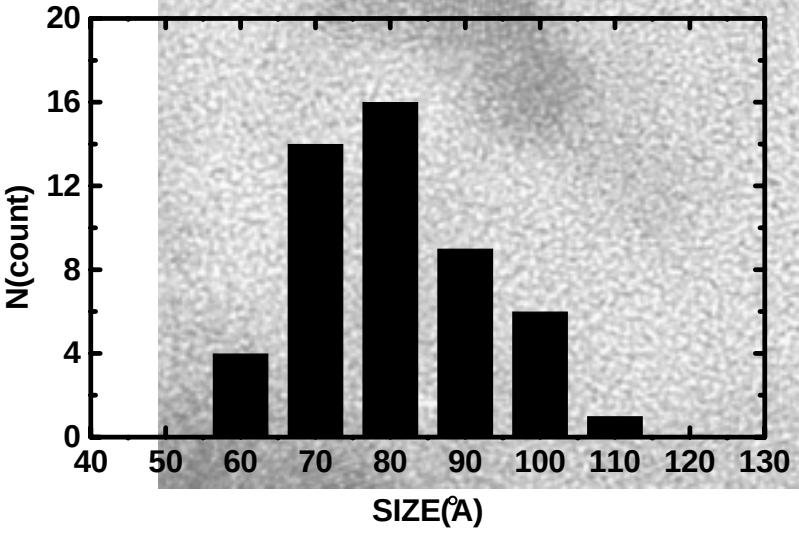

Fracture stress enhanced from 0.56 GPa (50-150 um grain Ironto 2.8 GPa)(40 nm grain)

Ductile region

Young's modulus

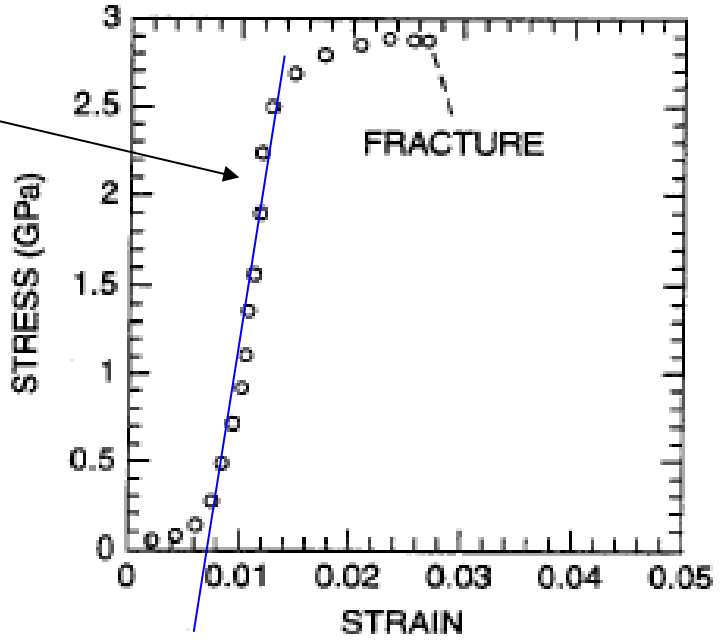

Ductile?柔軟
Brittle? 脆
elongation

ure 6.3. Stress–strain curve for bulk compacted nanostructured Fe–Cu material, showing ture at a stress of 2.8 GPa. [Adapted from L. He and E. Ma, *J. Mater. Res.* **15**, 904 (2000).]

Rapid solidfication-Chill block melt spinning

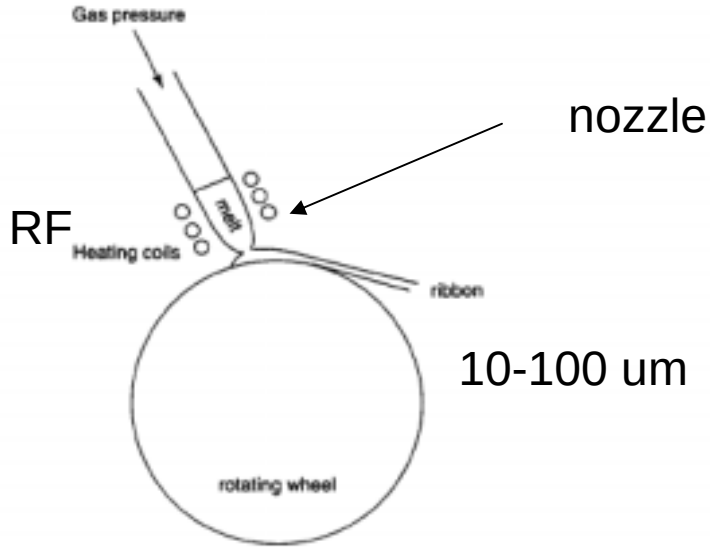

Figure 6.4. Illustration of the chill block melting apparatus for producing nanostructured materials by rapid solidification on a rotating wheel. (With permission from I. Chang, in *Handbook of Nanostructured Materials and Nanotechnology*, H. S. Nalwa, ed., Academic Press, San Diego, 2000, Vol. 1, Chapter 11, p. 501.)

- Light weight, high strength materials
- 1. A melt spun alloy Al(85-94%)-Y-Ni-Fe
- 2. Consisting of 10-30 nm Al particles embedded
- 3. Tensile strength ~1.2 GPa
- 4. Defect free aluminum nanoparticles

Gas atomization

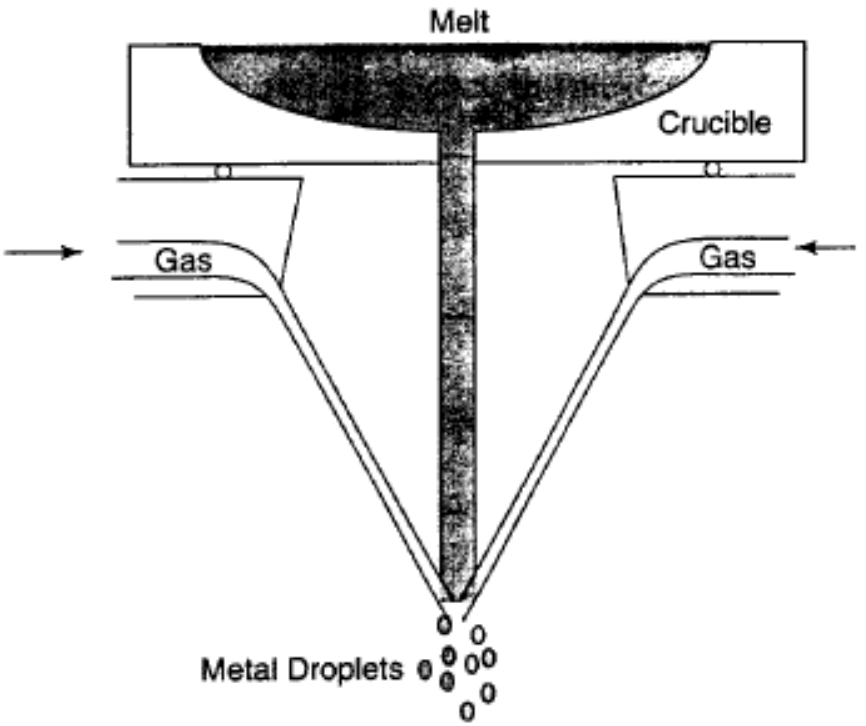

Figure 6.5. Illustration of apparatus for making droplets of metal nanoparticles by gas atomization. (With permission from I. Chang, in *Handbook of Nanostructured Materials and Nanotechnology*, H. S. Nalwa, ed., Academic Press, San Diego, 2000, Vol. 1, Chapter 11, p. 501.)

Electrodeposition

- Electrodes： Titanium
- Electrolyte ： $CuSo_4$(電解液)
- Cu 2 mm film (-Titanium)with grain size of 27 nm
- Enhanced yield strength 119 MPa

6.1.2 Failure mechanisms of conventional grain-sized materials

Crack!

An irreversible elongation after breaking of the bond

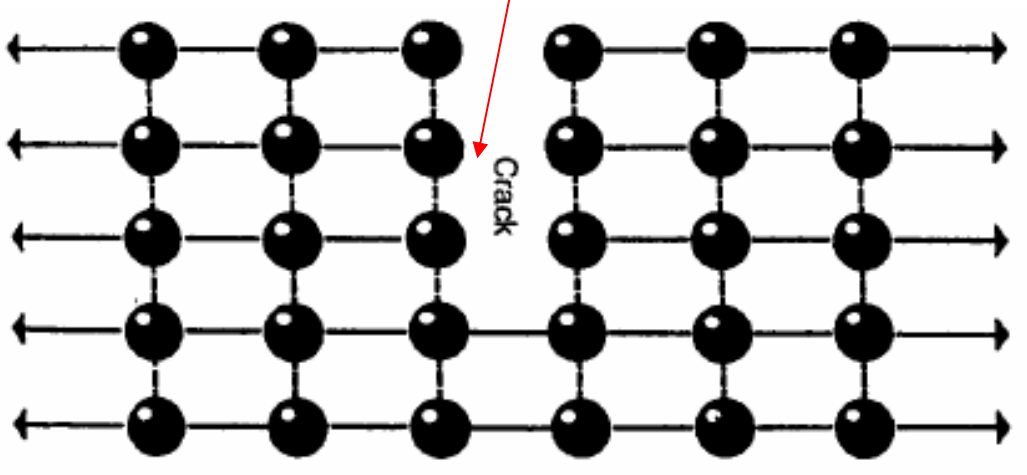

Figure 6.6. A crack in a two-dimensional rectangular lattice.

Brittle to ductile transition !

B to D region

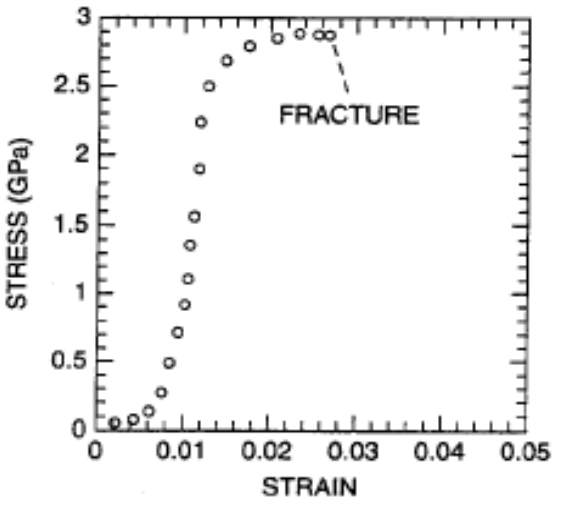

-strain curve for bulk compacted nanostructured Fe-
of 2.8 GPa. [Adapted from L. He and E. Ma, *J. Mater.*

Lattice dislocation.

1. Lattice slide
2. Weaker bonds along the dislocation

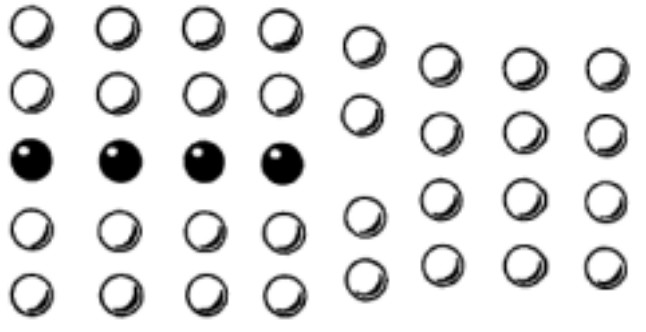

Figure 6.7. An edge dislocation in a two-dimensional rectangular lattice.

Hardening: to Impede the movement of dislocation by introducing tiny particles iron carbide into steel

6.1.3 Mechanical Properties

that below ~20 nm, Young's modulus begins to decrease from its value in conventional grain-sized materials.

The larger the value of Young's modulus, the less elastic the material.

Young's modulus
stress-strain ratio

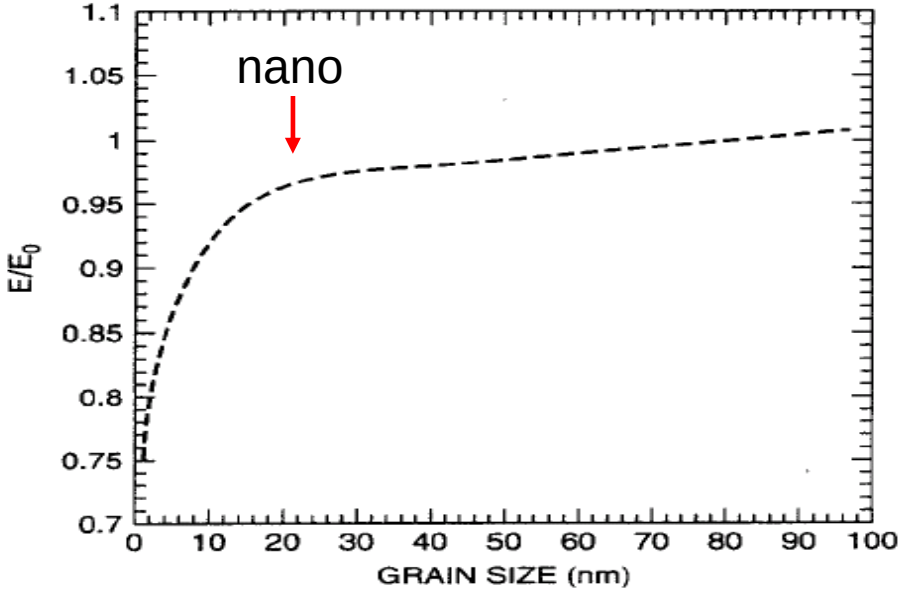

Plot of the ratio of Young's modulus *E* in nanograin iron to its granular iron as a function of grain size.

Hall-Petch equation

For convention grain

Yield strength

$\sigma = \sigma_0 + K / d^{1/2}$

- Materials having smaller grains have more grain boundaries, blocking dislocation movement

- Bulk nanostructured materials are quite brittle and display reduced ductility (~ a few % elongations) for grain size < 30 nm. Due to flaws and porosity
- As compared to copper (60% elongations)

Most bulk nanostructured materials are quite brittle and display reduced ductility

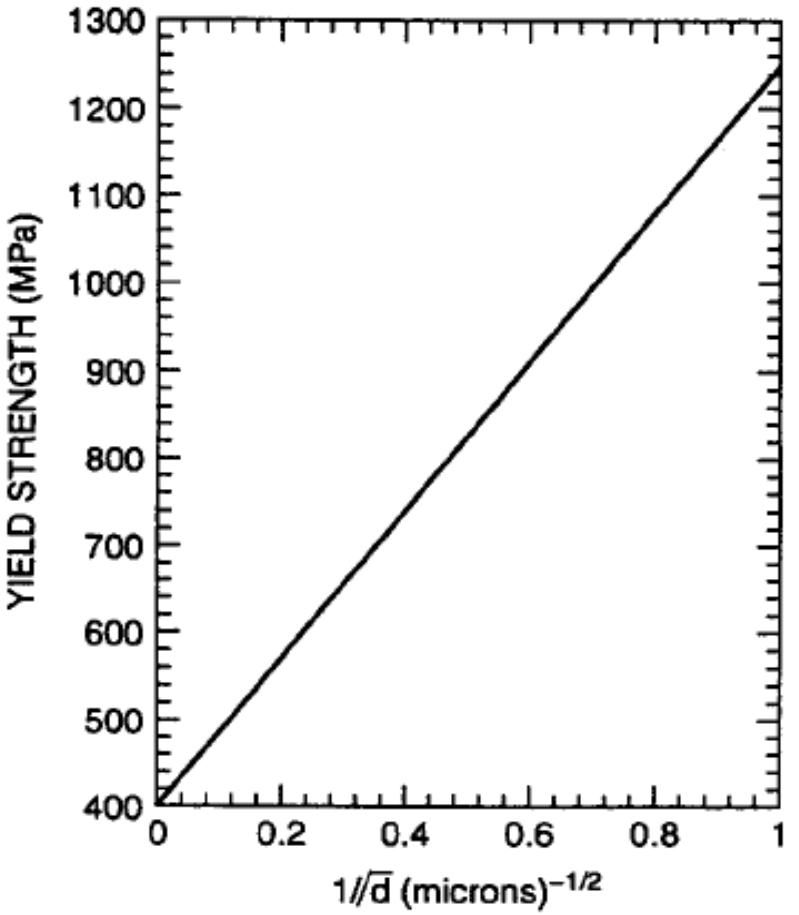

strength of Fe–Co alloys versus $1/d^{1/2}$, where d is the size

6.1.4 Nanostructured multilayers

the planar boundary between two layers is very high. For example, a square centimeter of a 1-μm-thick multilayer film having layers of 2 nm thickness has an interface area of 1000 cm^2. Since the material has a density of about 6.5 g/cm^3, the interface area density is 154 m^2/g, comparable to that of typical heterogeneous properties of these materials. These layered materials have very high hardness,

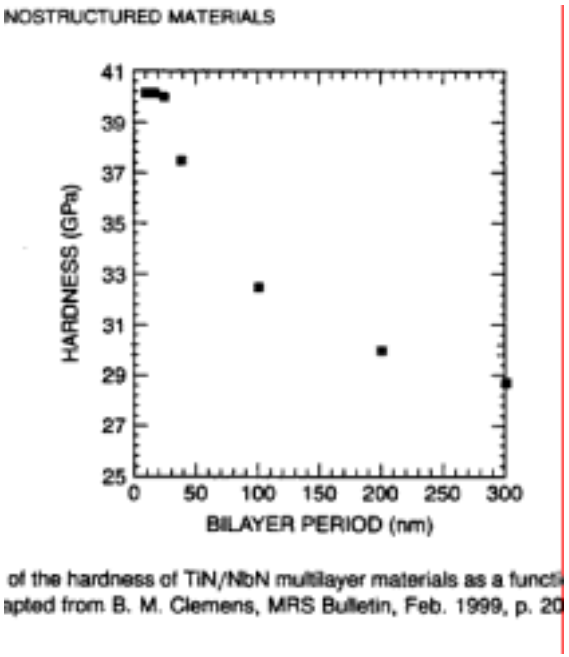

of the hardness of TiN/NbN multilayer materials as a functi
apted from B. M. Clemens, MRS Bulletin, Feb. 1999, p. 20

Mismatch of crystal structure
TiN a=0.4235 nm
NbN a=0.5151 nm

nanoindenter

6.1.5 Electrical properties

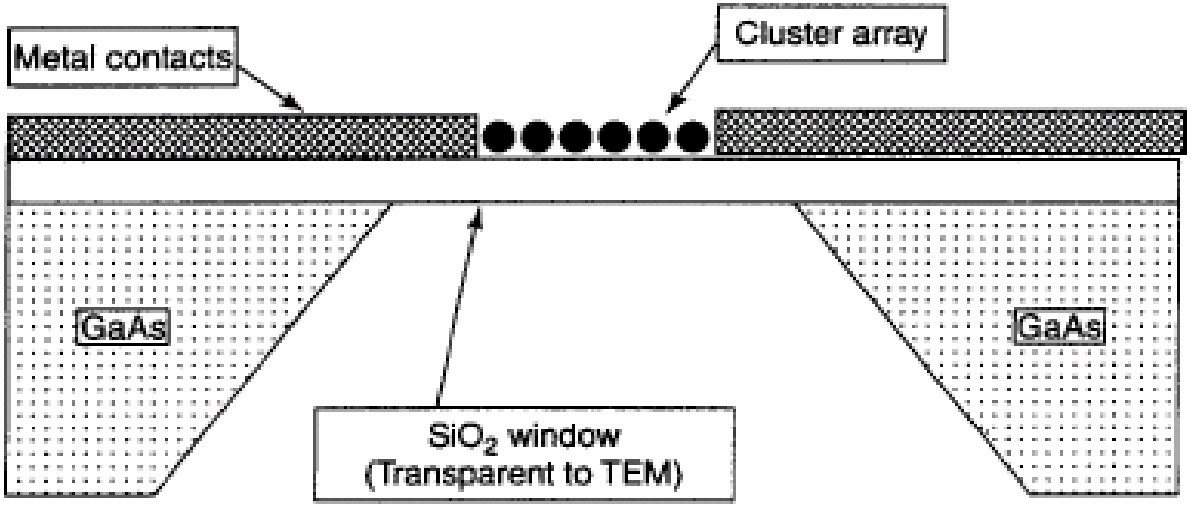

Figure 6.12. Cross-sectional view of a lithographically fabricated device to measure the electrical conductivity in a two-dimensional array of gold nanoparticles linked by molecules. (With permission from R. P Andres et al., in *Handbook of Nanostructured Materials and Nanotechnology*, H. S. Nalwa, ed., Academic Press, San Diego, 2000, Vol. 3, Chapter 4, p. 217.

E: activation energy

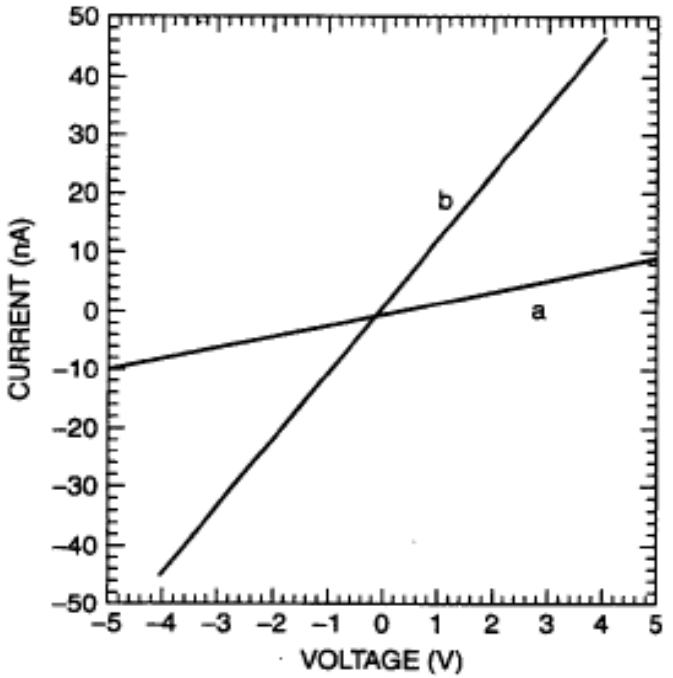

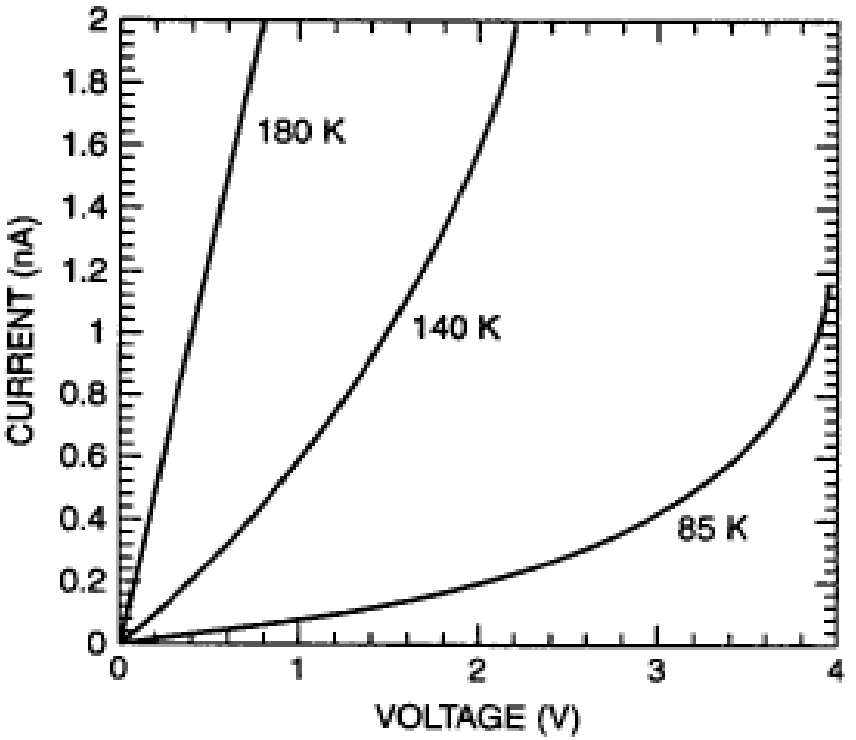

oom-temperature current–voltage relationship for a two-dimen
kage (line a) and with the particles linked by a $(CN)_2C_{18}H_{12}$ molecule (line b).

$$G = G_o \exp\left(\frac{-E}{k_B T}\right)$$

Electron tunneling

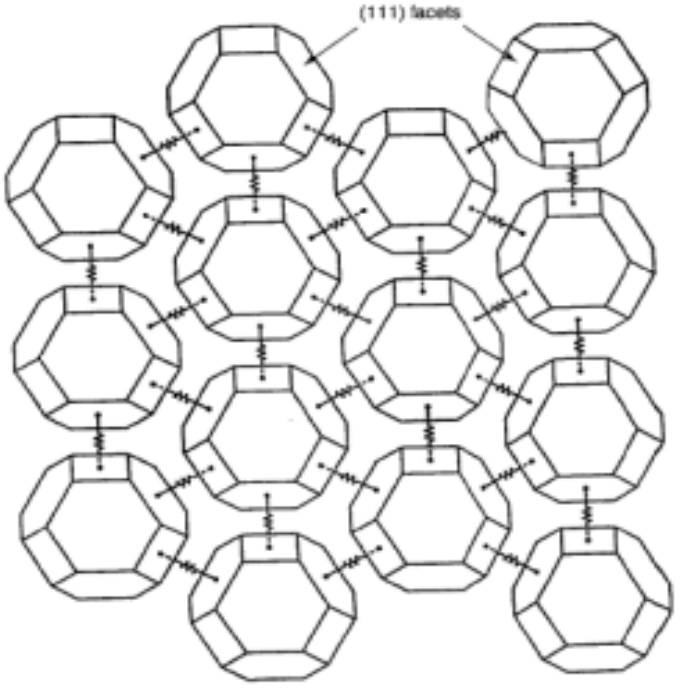

Figure 6.15. Sketch of a model to explain the electrical conductivity in an ideal hexagonal array of single-crystal gold clusters with uniform intercluster resistive linkage provided by resistors

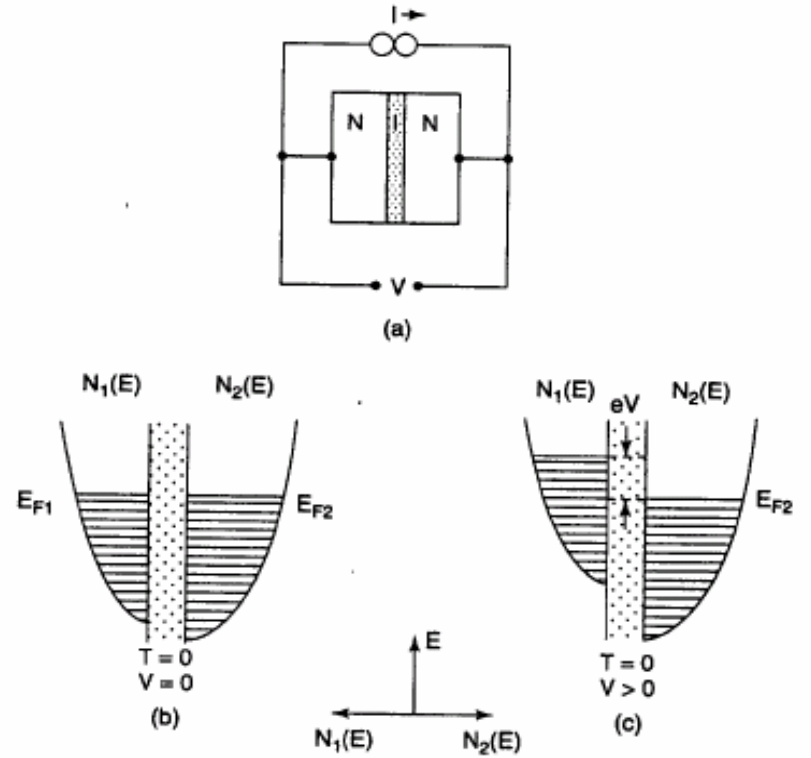

.16. (a) Metal–insulator–metal junction; (b) density of states of occupied leve

$$N_1(E - \mathrm{eV}) f(E - \mathrm{eV})[N_2(E)(1 - f(E))] \qquad (6.3)$$

The no. of electrons that can move

$$I = K \int N_1(E - \mathrm{eV}) N_2(E)[f(E - \mathrm{eV}) - f(E)]dE \qquad (6.4)$$

Net Current

$$I = KN_1(E_f)N_2(E_f)\mathrm{eV}$$

$$G_{nn} = KN_1(E_f)N_2(E_f)e \qquad (6.7)$$

6.1.8 Porous Silicon made by electrochemical etching in hydrogen fluoride

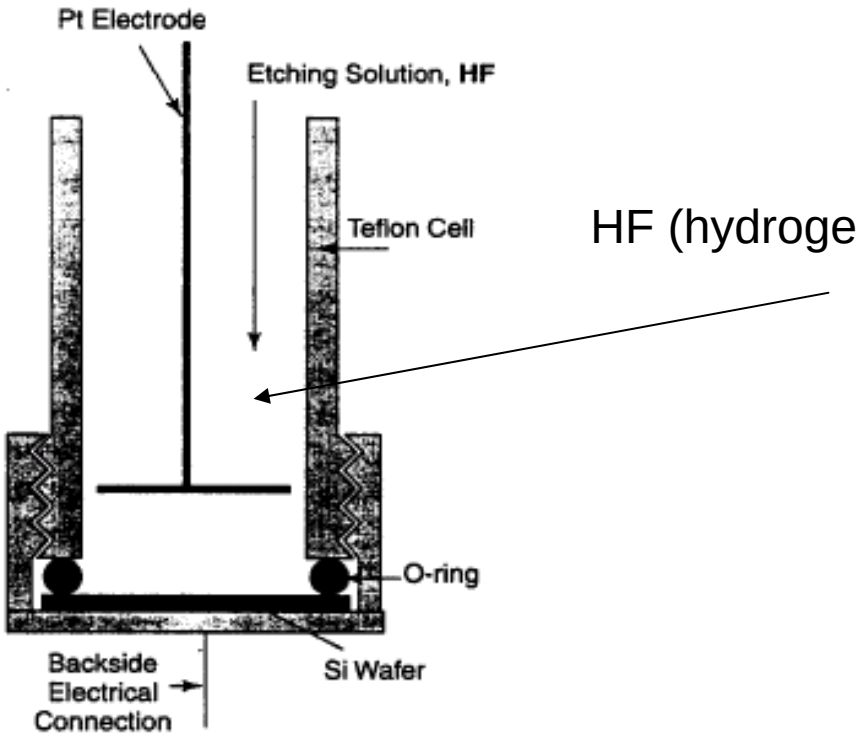

HF (hydrogen fluoride)

6.21. A cell for etching a silicon wafer in a hydrogen fluoride (HF) solution in order to ce pores. (With permission from D. F. Thomas et al., in *Handbook of Nanostructured ls and Nanotechnology*, H. S. Nalwa, ed., Academic Press, San Diego, 2000, Vol. 4, r 3, p. 173.)

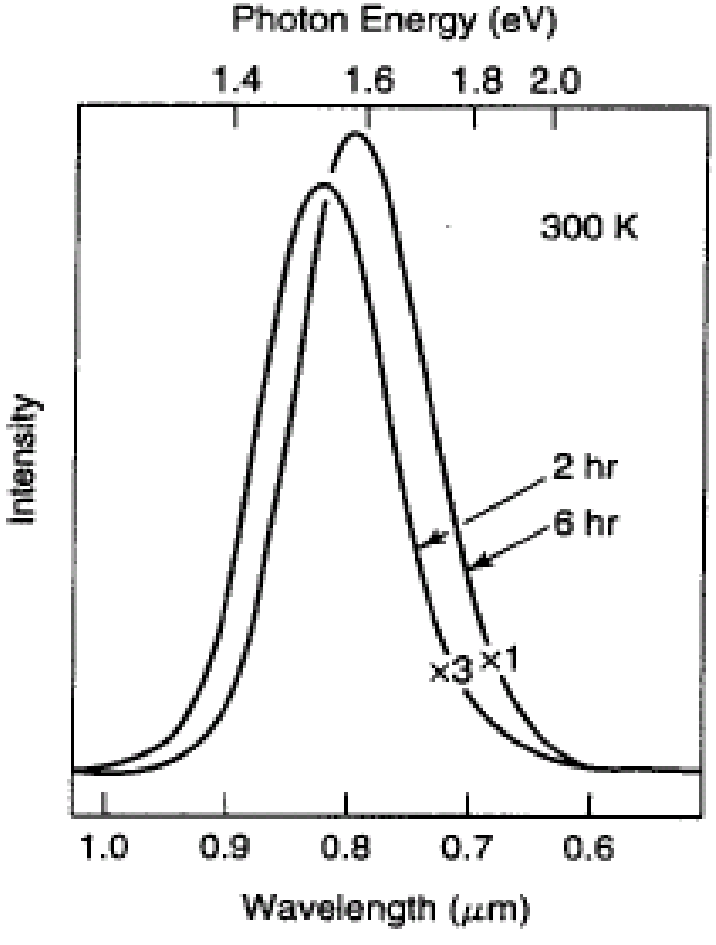

uminescence spectra of porous silicon for two differe
lote the change in scale for the two curves. [Adapted f

Luminescence: Absorption of energy
Reemit Visible or near-visible light

Fluorescence: emission occurs within 10^{-8} s

Phosphorescence: a delay emission

Explanations

p-type silicon is etched, a very fine network of pores having dimensions less than 10 nm is produced.

A number of explanations have been offered to explain the origin of the fluorescence of porous silicon, such as the presence of oxides on the surface of the pores that emit molecular fluorescence, surface defect states, quantum wires, quantum dots and the resulting quantum confinement, and surface states on quantum dots. Porous silicon also displays electroluminscence, whereby the luminescence is induced by the application of a small voltage across electrodes mounted on the silicon, and cathodoluminescence from bombarding electrons.

Quantum effects 量子效應 ：

Quantum size effect
「量子尺寸效應」

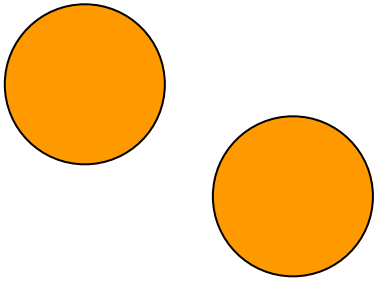

Particles,etc

Quantum confinement effect
「量子侷限效應」

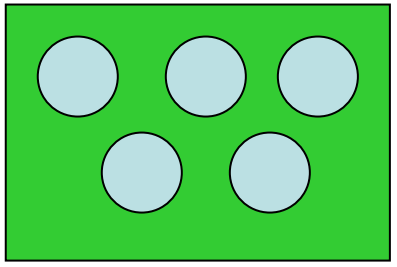

mesoporous materials,etc

Nanowire Growth Mechanism

- Vapor-Liquid-Solid
- Melt injection into porous templates
- ✓ Electrodeposition into porous templates

Fabrication of Porous Anodic Alumina Templates

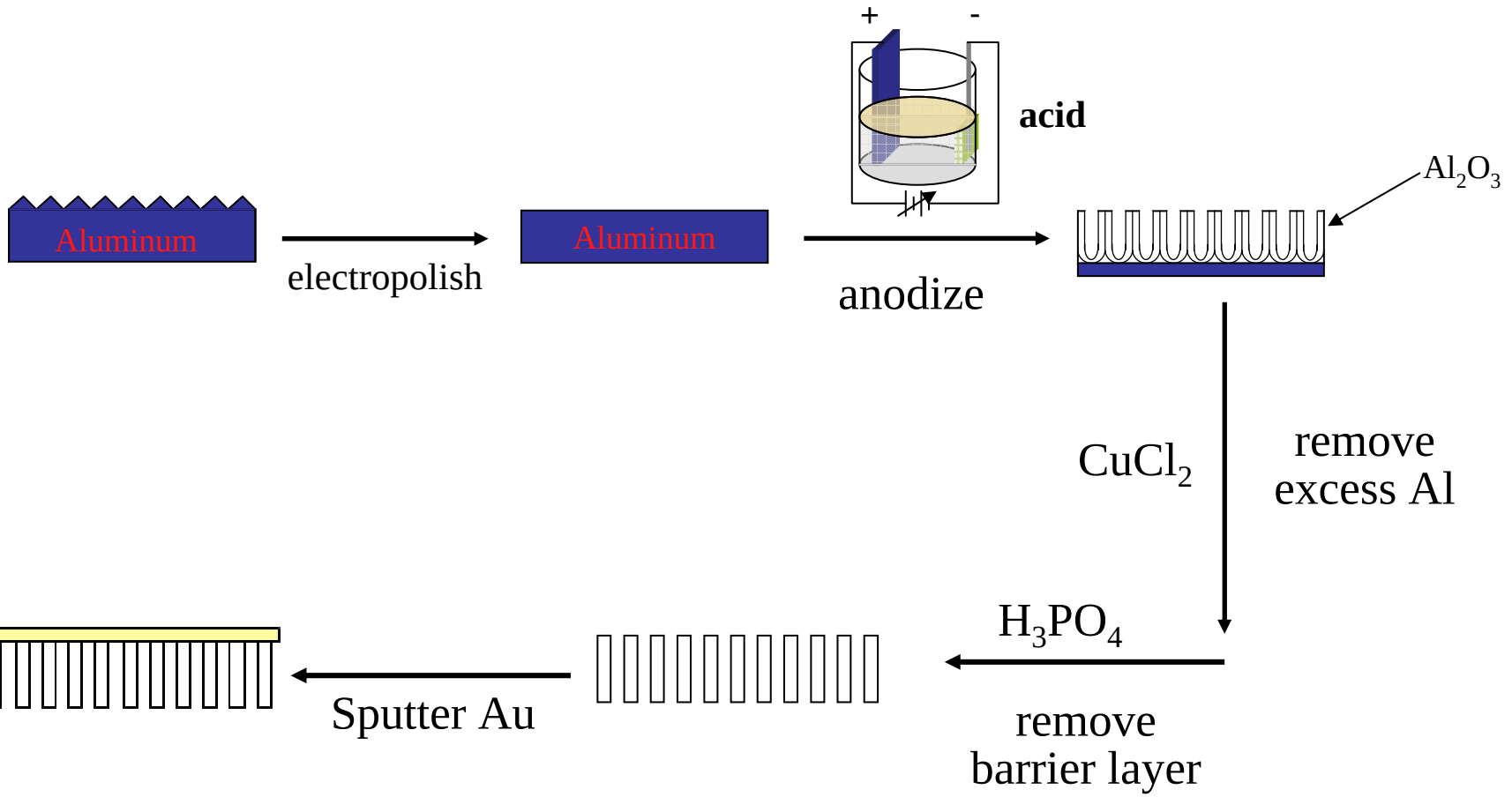

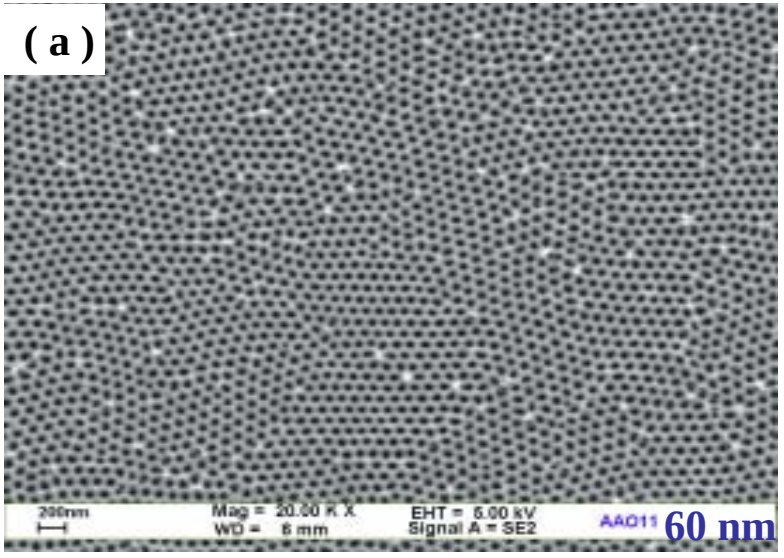

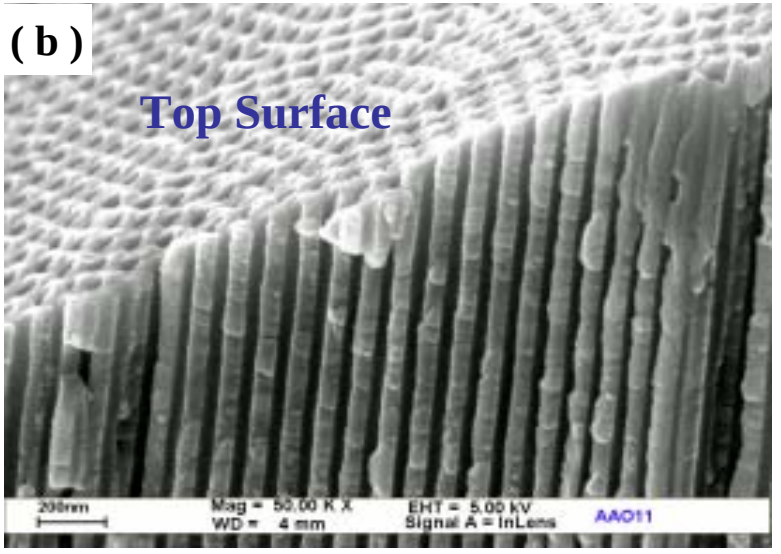

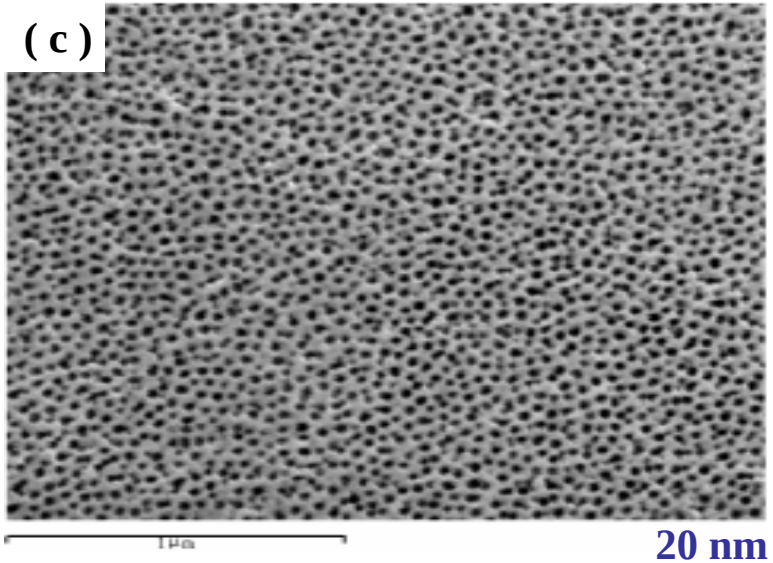

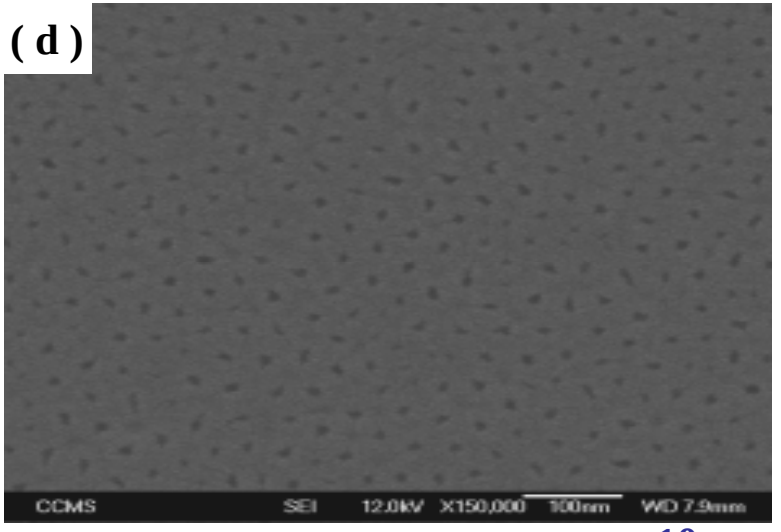

利用陽極處理氧化鋁 (Anodic Aluminum Oxide, AAO)製造各式尺寸的奈米孔洞模板, 孔洞的直徑分別為圖(a) 60nm (b)60nm nanopore template 的側面圖. (c)20nm (d) 10nm.

Electrodeposition of Bi2Te3 nanowire arrays

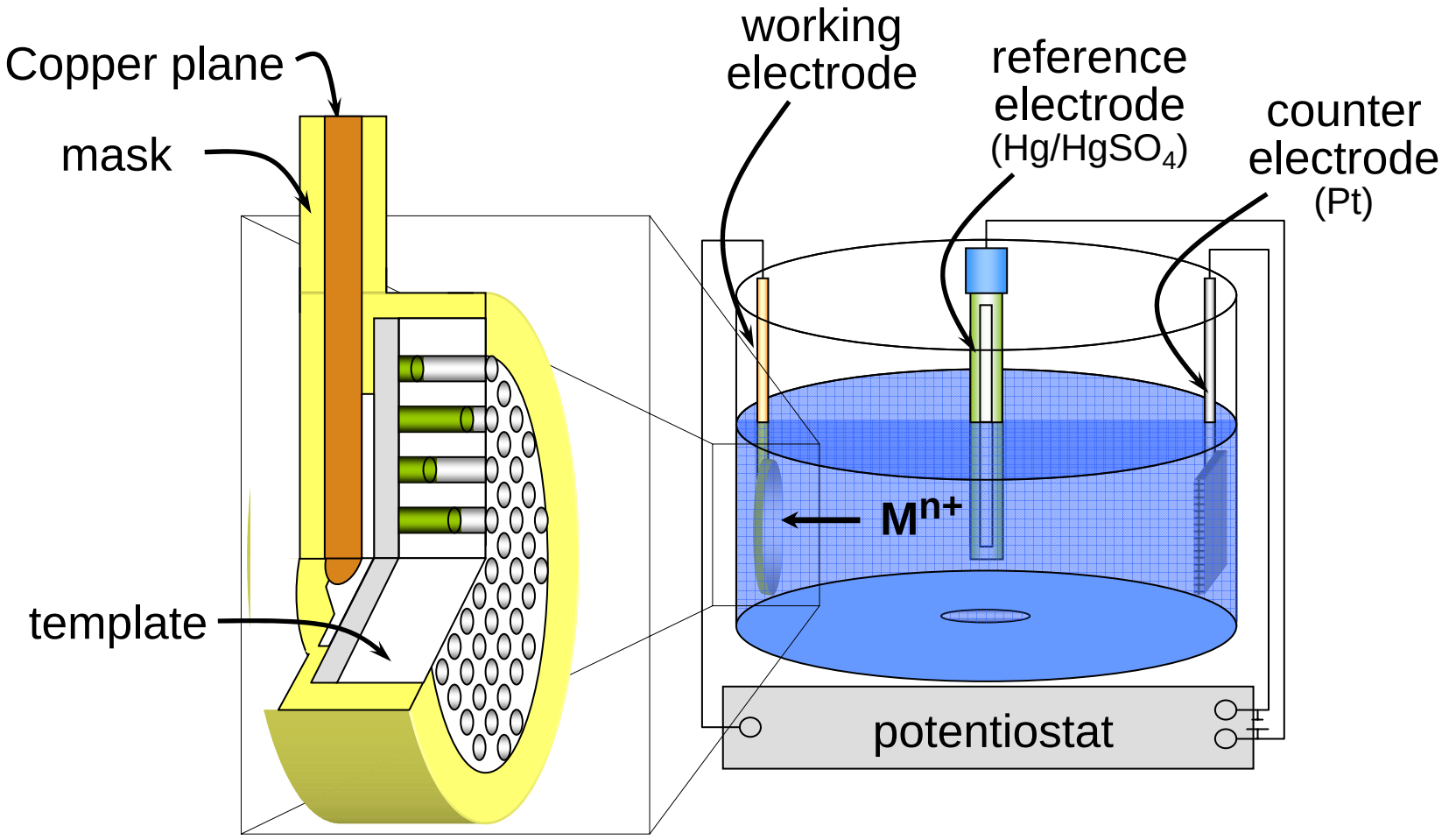

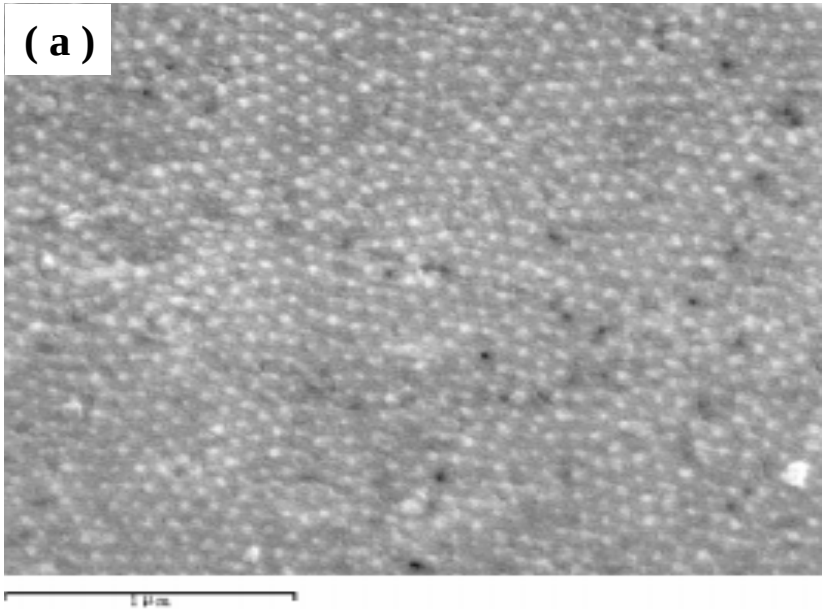
(a)
1 µm

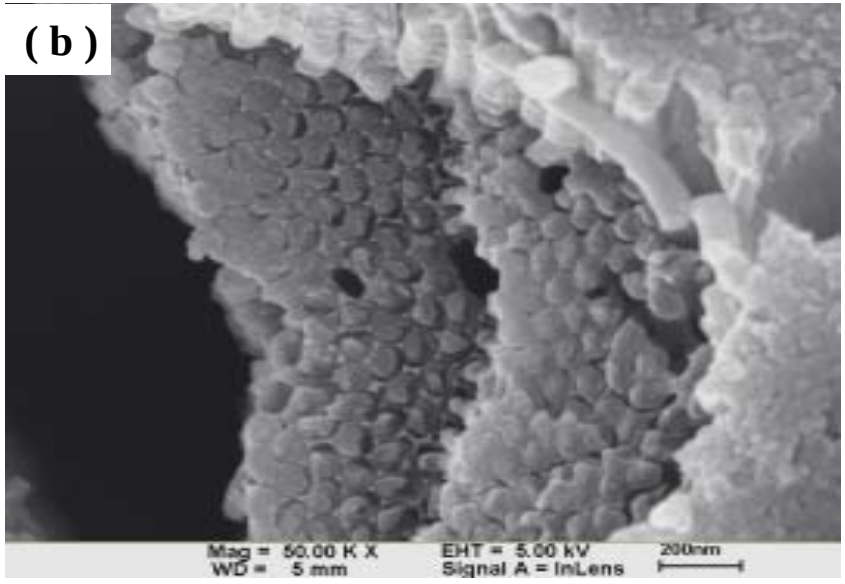
(b)
Mag = 50.00 K X
WD = 5 mm
EHT = 5.00 kV
Signal A = InLens
200nm

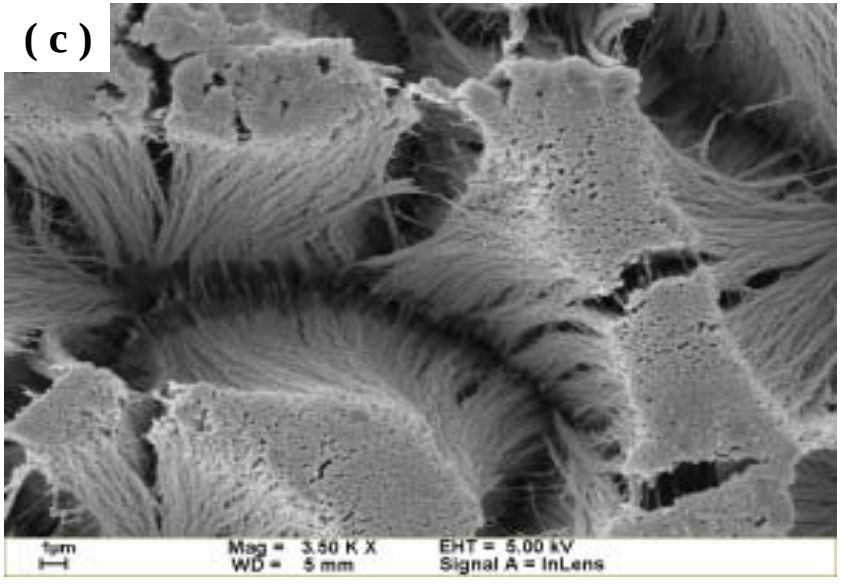
(c)
1µm
Mag = 3.50 K X
WD = 5 mm
EHT = 5.00 kV
Signal A = InLens


(d)
100 nm

Synthesis of Bi_2Te_3/alumina nanocomposites

UC, Berkley

Empty template - 75 nm pore diameter

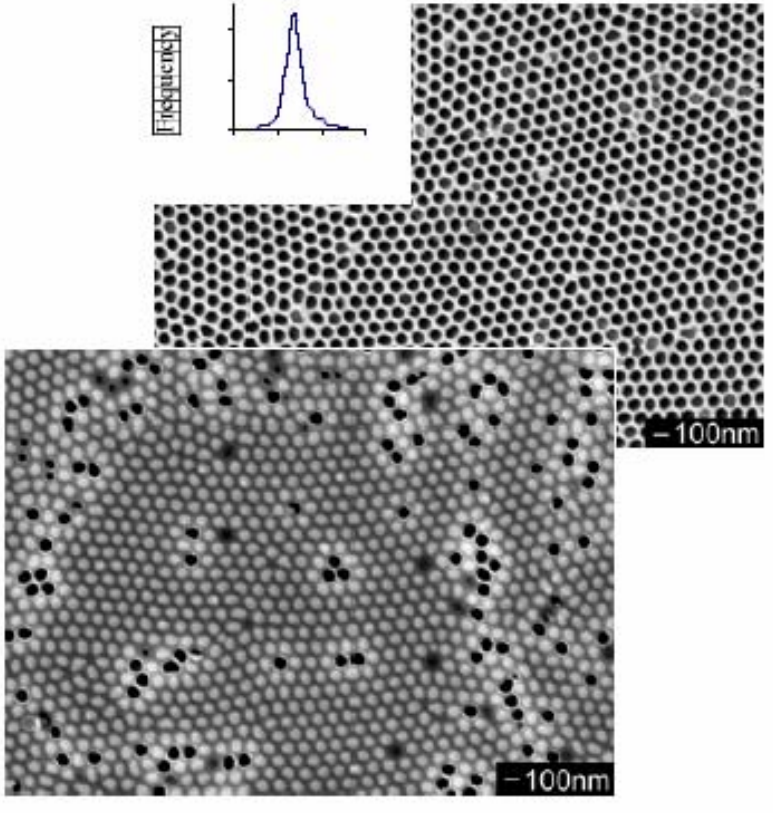

Empty template - 25 nm pore diameter

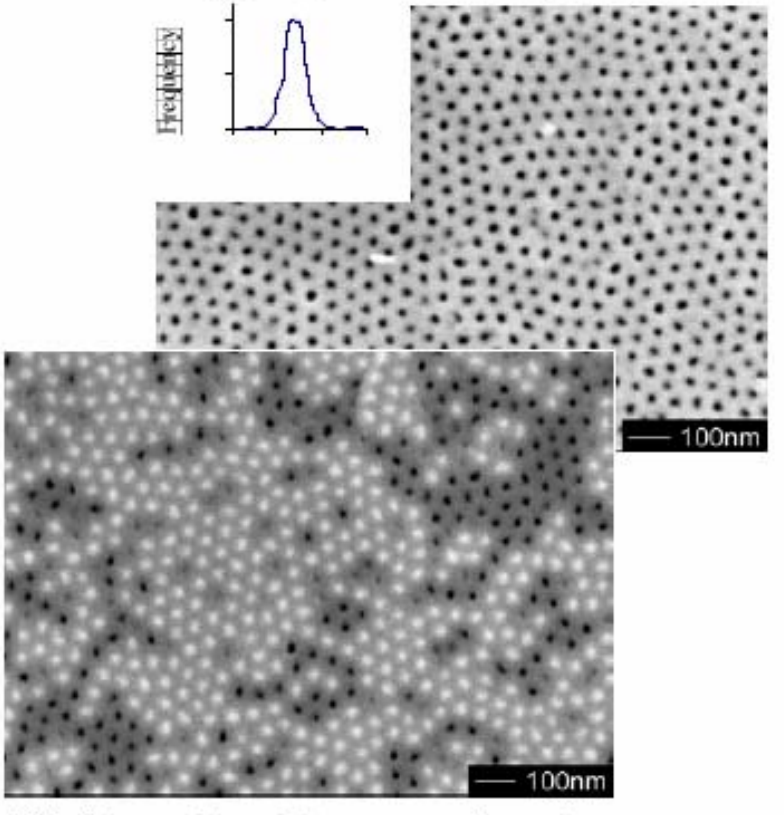

Filled template - 75 nm pore diameter

Filled template - 25 nm pore diameter

M.S. Sander, R. Gronsky, T. Sands, A.M. Stacy, "Structure of Bismuth Telluride Nanowire Arrays fabricated by Electrodeposition into Porous Anodic Alumina Templates," *Chem. Mater.* **15** (2003) pp. 335-39

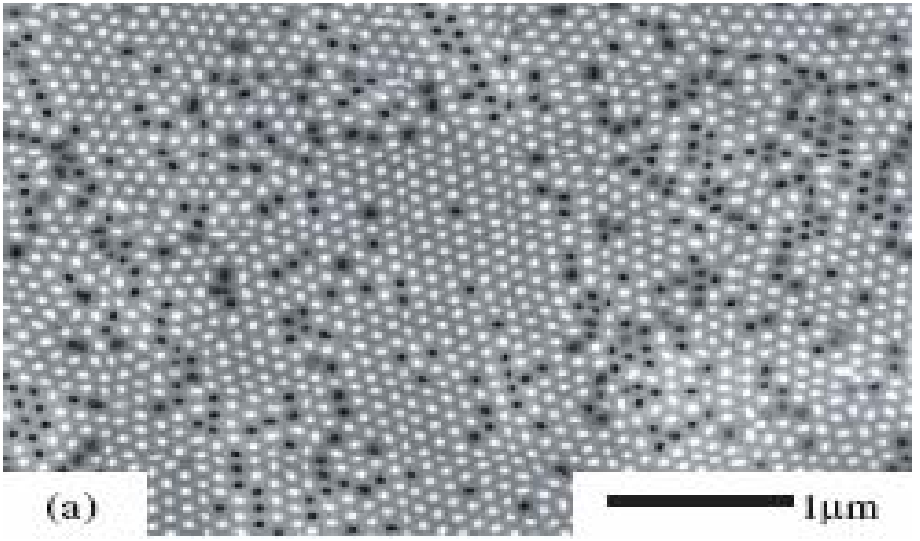

Bi2Te3 nanowire arrays (~45 nm)

(A. M. Stacy. Group, U. C. Berkeley. 2002)

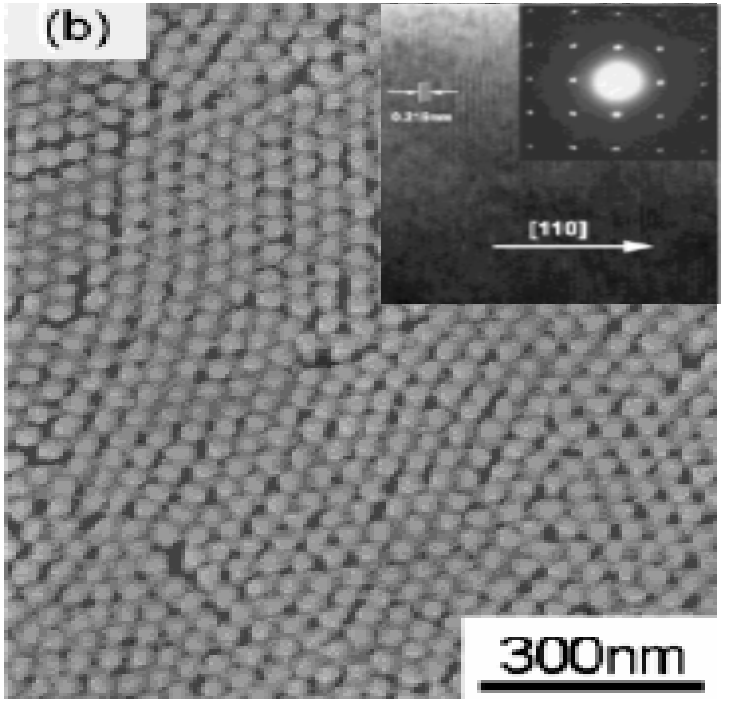

Hexagonal Bi2Te3 single-crystal Nanowires.

(Xiaoguang Li, *Hefei*, P. R. China)

J. Phys. Chem. B **2004,** *108,* 1844-1847

6.2 Nanostuctured Crystals

- Natural Nanocrystal
- B12

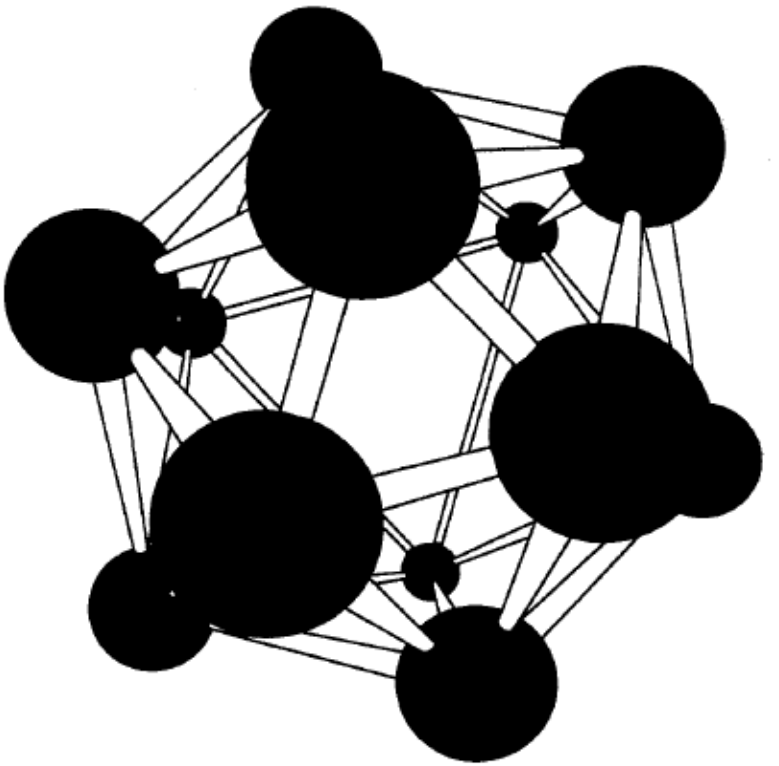

ıre 6.22. The icosohedral structure of a boron cluster containing 12 atoms. This
ɔasic unit of a number of boron lattices.

Fullerence C60

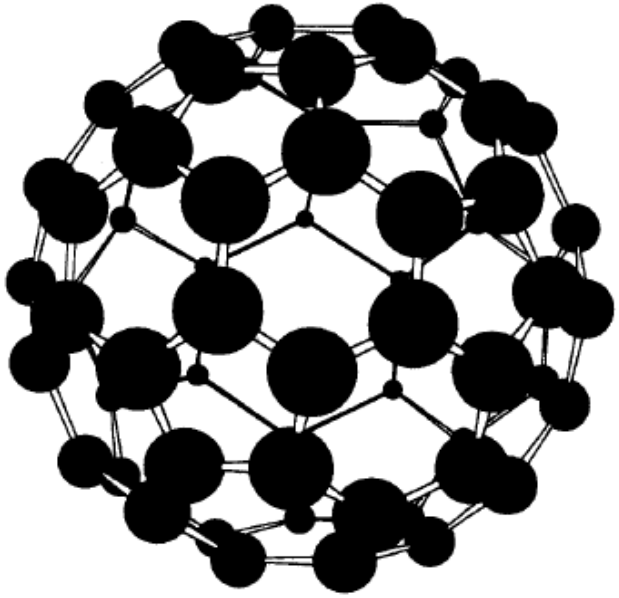

Figure 5.6. Structure of the C_{60} fullerene molecule.

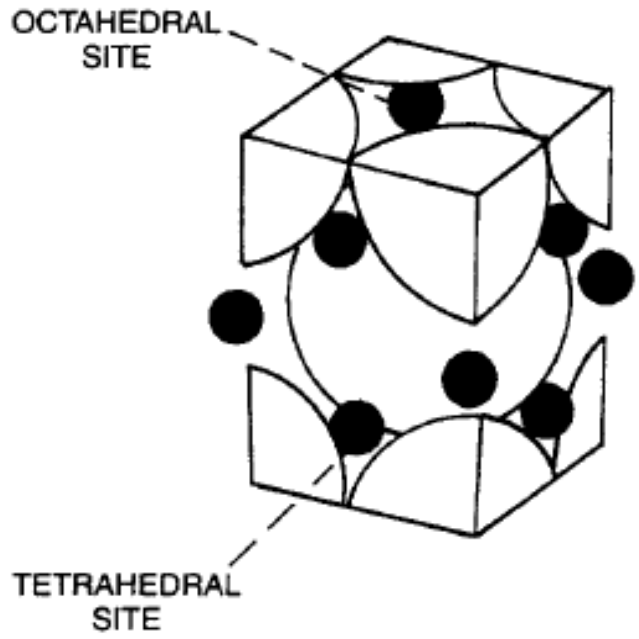

ystal lattice unit cell of C_{60} molecules (large spheres) doped with alkali atoms

6.2.3 Arrays of nanoparticles in Zeolites

- Zeolites: Cubic mineral
- $(Na_2,Ca)Al_2Si_4)O_{12}.8H_20$
- Porous materials

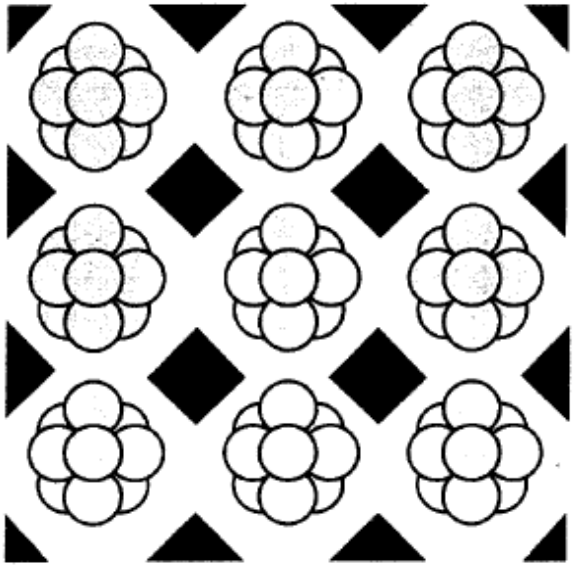

Schematic of cluster assemblies in zeolite pores. (With
ov et al., in *Handbook of Nanostructured Materials and*
d., Academic Press, San Diego, 2000, Vol. 4, Chapter 4, p. 23

Zeolite--Mordenite

- $(Ca,Na,K_2)(Al_2Si_{10})O_{24}.7H_2O$
- Orthrorhombic
- Long parrel channels
- With d= 0.6 nm

- Se atoms fill into the channe
- to form chains of single atom

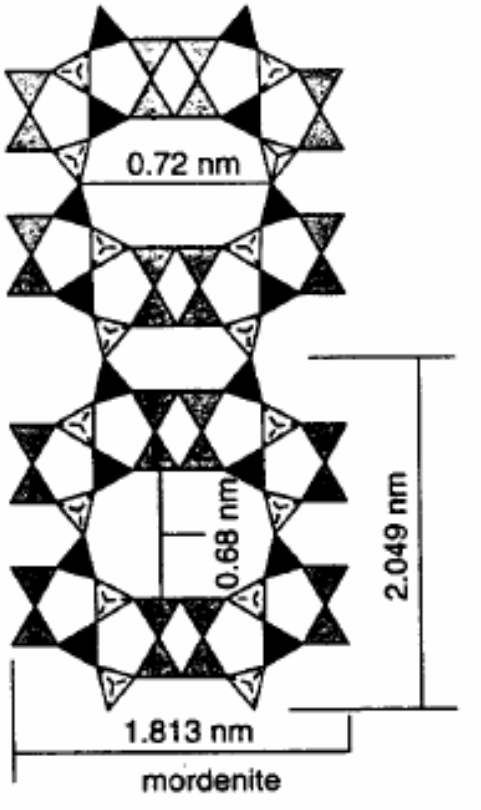

Optical absorption

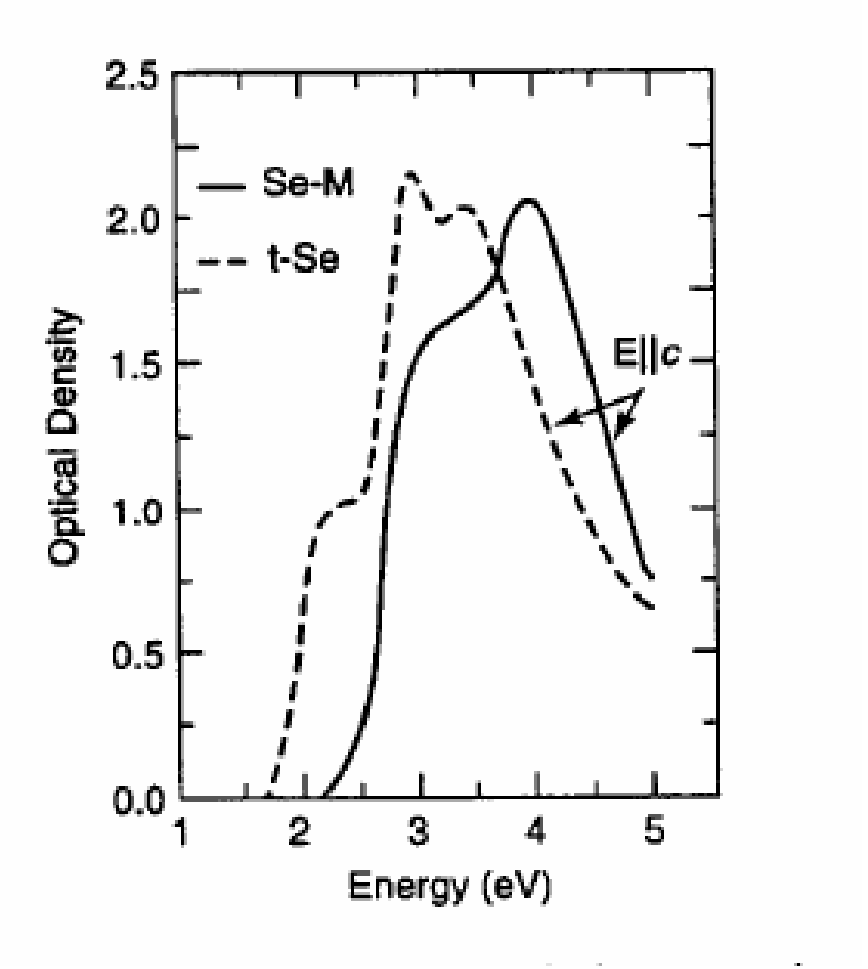

The electronic structure of Se chains is different from Se crystal

6.2.4 Crystals of metal nanoparticles

Chemical reduction !

6.2.4. Crystals of Metal Nanoparticles

A two-phase water toluene reduction of $AuCl_4^-$ by sodium borohydride in the presence of an alkanethiol ($C_{12}H_{25}SH$) solution produces gold nanoparticles Au_m having a surface coating of thiol, and embedded in an organic compound. The overall reaction scheme is

$$AuCl_4^-(aq) + N(C_8H_{17})_4 + (C_6H_5Me) \rightarrow N(C_8H_{17})_4 + AuCl_4^-(C_6H_5Me) \quad (6.10)$$

$$m AuCl_4^-(C_6H_5Me) + n(C_{12}H_{25}SH)(C_6H_5Me) + 3me^- \rightarrow 4mCl^-(aq) + (Au_m)(C_{12}H_{25}SH)_n(C_6H_5Me) \quad (6.11)$$

6.2.6 Photonic Crystals

The wavefunction of an electron in a metal can be written in the free-electron approximation as

$$\Psi_{k[r]} = \left[\frac{1}{V}\right]^{1/3} e^{ik\cdot r} \qquad (6.12)$$

$E=h^2k^2/8\pi^2m$

Bragg reflection

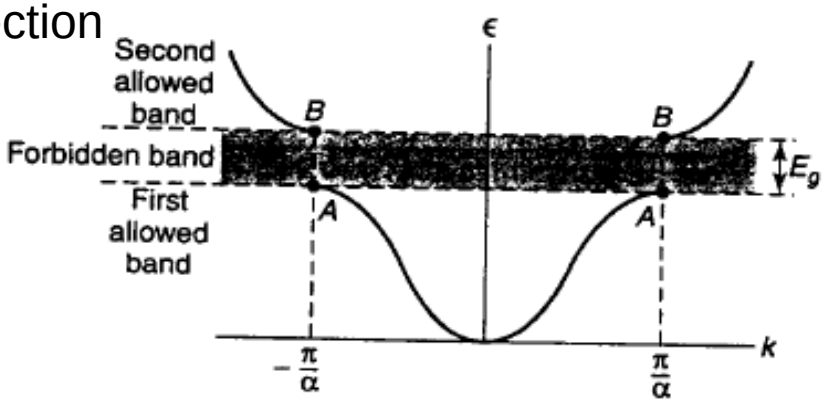

Figure 6.29. Curve of energy *E* plotted versus wavevector *k* for a one-dimensional line of atoms.

there is an energy gap. This is a result of the lattice periodicity and the wave nature of the electrons.

1987 Yablonovitch Bragg reflection for light in the building lattice

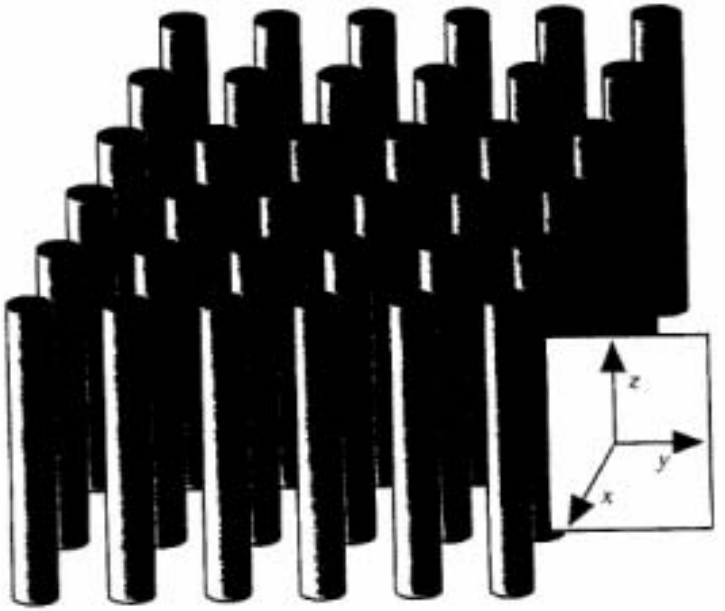

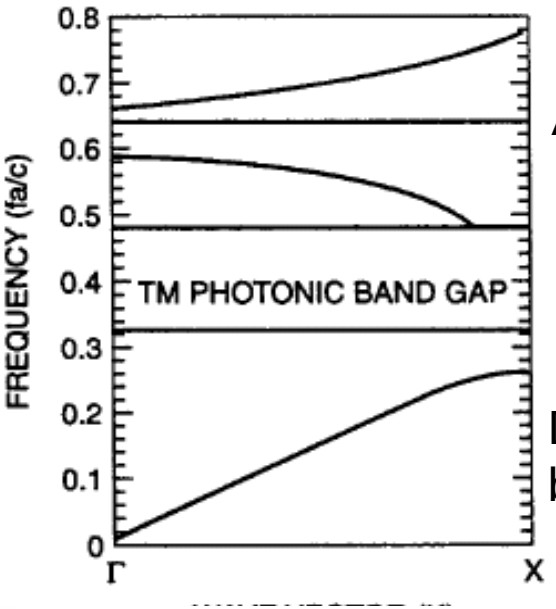

Air band

Dielectric band

6.30. A two-dimensional photonic crystal made by arranging long cylinders of dielectric ils in a square lattice array.

$(Al_2O_3,\ \varepsilon = 8.9)$ d=0.37 mm l=100mm s=1.97 mm

Maxwell's equations in a periodic dielectric structure. The associated Helmholtz equation obtained for the case of no external current sources is

$$\nabla^2 H(r) + \varepsilon\left[\frac{\omega^2}{c^2}\right] H(r) = 0 \qquad (6.13)$$

Wave guide

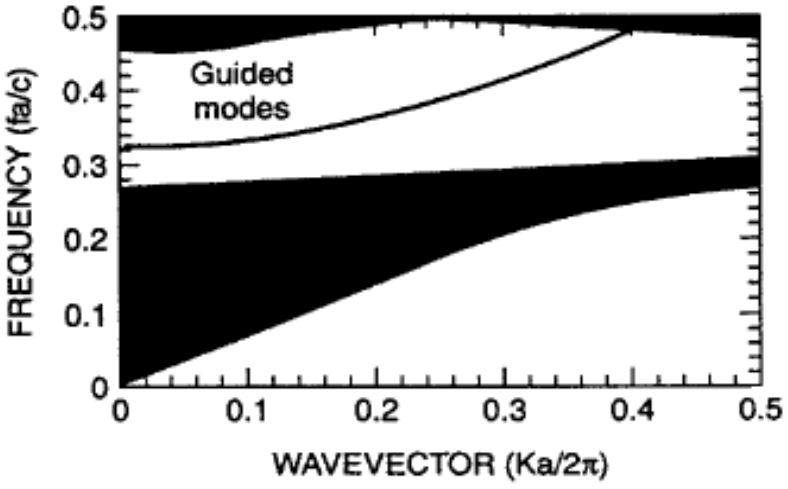

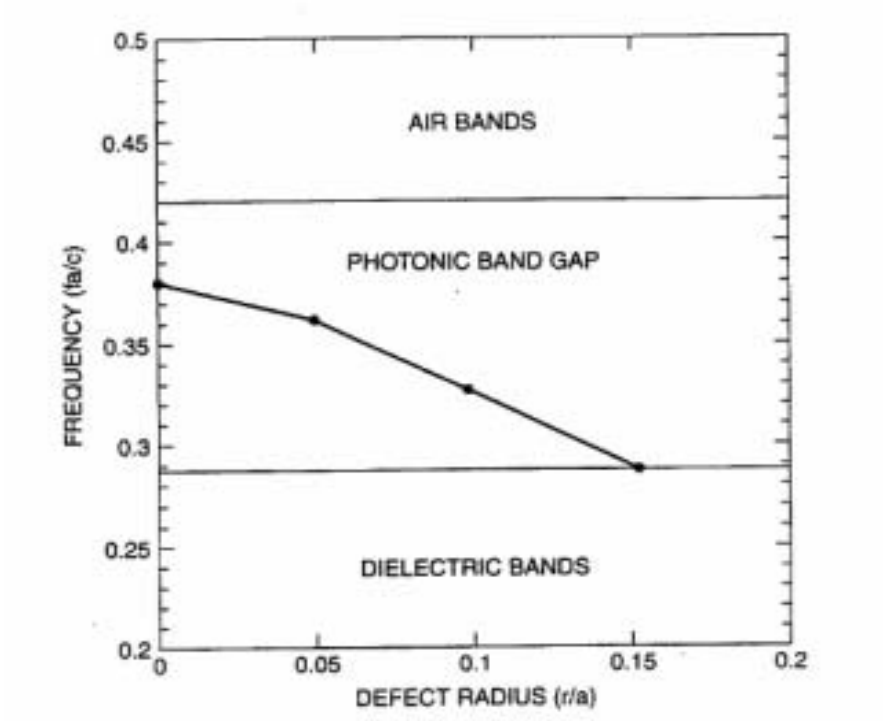

e 6.33. Dependence of frequency of localized states in the band gap formed on the r